INTERNATIONAL JOURNAL OF CLIMATOLOGY
Int. J. Climatol. **26**: 897–913 (2006)
Published online 27 March 2006 in Wiley InterScience (www.interscience.wiley.com). DOI: 10.1002/joc.1292

EVIDENCE FOR INFLUENCE OF ANTHROPOGENIC SURFACE PROCESSES ON LOWER TROPOSPHERIC AND SURFACE TEMPERATURE TRENDS

A. T. J. DE LAAT* and A. N. MAURELLIS
Netherlands Institute for Space Research (SRON), EOS, Utrecht, Netherlands

Received 31 October 2005
Revised 31 October 2005
Accepted 2 November 2005

ABSTRACT

In de Laat and Maurellis (2004), a new framework was introduced in the form of a spatial-thresholding trend technique for analyzing the correlation between anthropogenic surface processes (e.g. changes in land use, albedo, soil moisture, groundwater levels, solar absorption by soot or energy consumption) and lower tropospheric and surface temperature trends for the period 1979–2001. *In situ* measured surface and satellite-measured lower tropospheric temperature trends were shown to be higher in the vicinity of industrialized regions, while such higher trends were not found in enhanced greenhouse gas (GHG) climate model simulations of temperature. It was suggested that surface and lower tropospheric temperature trends appeared to be influenced by anthropogenic non-GHG processes on the earth's surface.

In this paper, we verify the robustness of the thresholding technique and confirm our earlier conclusions on the basis of an extended analysis and two additional data sets. We confirm the presence of a temperature change–industrialization correlation by analyzing the data with an additional statistical method and further confirm the absence of the above correlation in climate model simulations of enhanced GHG warming. Our findings thus provide an important test of climate model performance on regional scales.

These findings suggest that over the last two decades non-GHG anthropogenic processes have also contributed significantly to surface temperature changes. We identify one process that potentially could contribute to the observed temperature patterns, although there certainly may be other processes involved. Copyright © 2006 Royal Meteorological Society.

KEY WORDS: temperature; climate change; surface processes; anthropogenic

1. INTRODUCTION

Current observational evidence shows that the surface of the earth has warmed considerably during the twentieth century (IPCC, 2001). Furthermore, global analyses of surface temperature records show that most of the warming that has occurred after 1980 is unexplained by known natural forcings (IPCC, 2001). Enhanced greenhouse gas (GHG) radiative forcing provides a plausible explanation, notwithstanding the fact that climate models have known limitations in their modeling of variability (to just name one recent climate model intercomparison study: Covey *et al*., 2003). On the other hand, less free tropospheric warming has occurred since 1980. Climate models and theory predict that enhanced GHG warming should occur throughout the troposphere (IPCC, 2001; Hansen *et al*., 2005; Santer *et al*., 2005; Chase *et al*., 2004). This discrepancy between surface and free tropospheric warming is a well-documented phenomenon (Bengtsson *et al*., 1999; Gaffen *et al*., 2000; Santer *et al*., 2000; IPCC, 2001; Lanzante *et al*., 2003; Seidel *et al*., 2004; Seidel and Lanzante, 2004; Pepin and Seidel, 2005). This discrepancy opens the possibility that other anthropogenic near-surface processes may have contributed to the observed surface temperature variations.

* Correspondence to: A. T. J. De Laat, Royal Dutch Meteorological Institute (KNMI), PO Box 201, 3730 AE De Bilt, The Netherlands; e-mail: jos.delaat@gmail.com

In de Laat and Maurellis (2004; hereafter Paper I), we showed that temperature trends at the surface and in the troposphere are spatially correlated with anthropogenic industrial CO_2 emissions. More specifically, temperature trends from satellite and *in situ* surface measurements, when compared to the CO_2 emissions for the period 1979–2001, showed that near-surface temperature trends are higher on average for regions with higher industrial CO_2 emissions. In contrast to our findings for the measurements, 'business-as-usual' climate model simulations of surface temperature changes due to increased GHG concentrations (used for IPCC (2001)) showed no such increase in trends for regions with higher emissions. This was not intended to suggest that a physical causality existed between the CO_2 emissions themselves and the temperature trends but rather intended to suggest that some underlying process, for which CO_2 emissions functioned as a proxy, was at work.

The existence of such surface warming processes would have important implications for our understanding of anthropogenic influence on climate and also for policy development to contain global warming. One of the goals of this paper is therefore to explore the robustness of the correlation between industrial CO_2 emissions and surface temperature changes. In other words, we show how much the findings of Paper I are the result of a real underlying, physical relationship rather than the spatial-thresholding method introduced in Paper I. The robustness of our findings is further supported by an analysis of other data sets using the spatial-thresholding method as well as other statistical tools.

In Section 2, we set out the principles of the spatial-thresholding method used in Paper I and extended here to other data sets. It should be noted that in the present work we introduce the use of area-weighted CO_2 emissions (which are a more accurate proxy for industrial activity – see Appendix 1) rather than total CO_2 emissions within a grid box (which we used in Paper I). In Section 3, we analyze two additional data sets (NCEP and ECMWF) similar to the analysis in Section 2. In Section 4, we test the robustness of the thresholding method using a bootstrapping method. We further test the robustness of the correlation between emissions and temperature trends using a direct comparison of the emissions and temperature trends and by exploring the spatial and temporal variations of the observed correlations. Section 5 starts with a summary of our findings and follows up with a discussion of the implications for future study of the influence of surface and lower tropospheric processes on climate.

2. METHOD AND INITIAL RESULTS: SPATIAL-THRESHOLDING TREND

As discussed in Paper I and throughout this work, we use a spatial-thresholding technique that operates as follows. First a particular value for industrial CO_2 emissions is chosen; this is the threshold. Temperature measurements (on a regular longitude–latitude grid) are then divided into two noncontiguous regions according to their corresponding CO_2 emissions value in the EDGAR database (Emissions Database for Global Atmospheric Research; van Aardenne *et al*., 2001): one region for which industrial CO_2 emissions exceed the threshold and one for which they do not. Mean temperatures and trends for all points in each of these two regions are then calculated by applying a linear regression to the monthly mean temperatures for the period 1979–2001. This procedure is repeated for the full range of industrial CO_2 emissions. The mean temperature trends for the above-threshold and below-threshold subregions are plotted (in this paper as red and blue points, respectively) against the value of the industrial CO_2 emissions threshold. This gives rise to the continuous curves shown in Paper I and onwards of Figure 1 in this work. The satellite data considered in Paper I were the Microwave Sounding Unit, (MSU) data from Christy *et al*. (2003) (University of Alabama, Huntington (UAH); middle and lower troposphere) and Mears *et al*. (2003) (Remote Sensing Systems (rss); middle troposphere), while the surface data was obtained from the Hadley Centre/Climate Research Unit (CRU) (Jones and Moberg, 2003). We note that the mean trends may be determined either: (1) by first calculating the trends and then averaging them or (2) by first calculating the average temperature and then the trend. Differences between both procedures were less than 2%. We chose the first approach since it also permitted a simple calculation of the 1-σ uncertainty for the trend of the mean temperatures. This uncertainty is denoted by the shaded areas around the curves. No measurement errors were taken into account in the 1-σ uncertainty calculations although we note temperature trend uncertainties due to measurement errors are 0.05 K/decade for the MSUuah satellite-measured temperature trends (Christy *et al*., 2003).

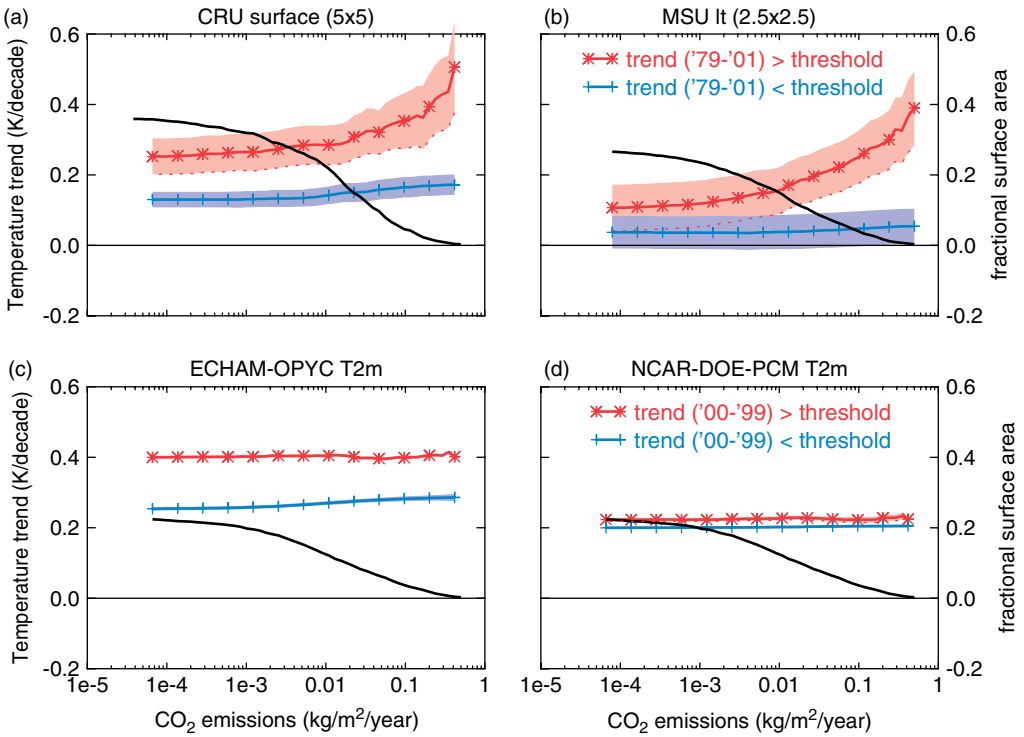

Figure 1. CO_2 emission–thresholded mean temperature trends (K/decade) covering the period 1979–2001 for measurements (a and b) and two models (c and d). Industrial surface CO_2 emissions are taken from the EDGAR 1990 database. The measurements include lower tropospheric MSU satellite temperature trends (MSUlt) and surface temperature trends from the Hadley Center/Climate Research Unit data set (CRU). Simulated 2-m temperatures are derived from NCAR-DOE-PCM and ECHAM4-OPYC3 climate models running the IPCC-IS92a emission scenario ('business as usual'). The shaded areas denote the mean 1-σ uncertainties of the linear regressions that do not include measurement errors. The additional black solid curve plotted in each panel denotes the fractional surface area of the earth for the above-threshold region. This figure is available in colour online at www.interscience.wiley.com/ijoc

The results of a thresholding analysis of two climate model simulations (NCAR-DOE-PCM and the ECHAM-OPYC) of enhanced GHG warming for 'business-as-usual' emission scenarios that have been used in IPCC (2001) are also shown in Figure 1. Note that 1-σ uncertainties in the trend calculations of the climate simulations are an order of magnitude smaller than measured uncertainties, indicating that these modeled temperature trends are very robust compared to modeled interannual variability.

The main conclusions that can be drawn from Figure 1 are that both satellite and surface data show a significant temperature increase with increasing emissions and that this correlation is absent in the climate models' temperature response.

It is also useful to note that the above-threshold (red (∗)) curves only reflect temperature trends over land, whereas the below-threshold (blue (+)) curves generally reflect a mixture of land and sea global temperature trends. This is because industrial emissions only occur over land. (The additional black solid curve plotted in each of Figures 1, 2, 6 and 7 denotes the fractional surface area of the earth for the above-threshold region.) Points at the extreme left-hand side of the above-threshold trends (red curves) correspond to the land mean temperature trend, while those lying on the extreme right-hand side of the below-threshold trend curves correspond to the global mean temperature trend of the data set under consideration.

What we have shown so far is that surface and satellite temperature data sets, though very different, give rise to very similar spatially thresholded trends patterns. On the one hand, the satellite data provide global coverage, but yet are more sensitive to free tropospheric temperature variations than to surface temperature trends (see Appendix 2). Surface temperature measurements, on the other hand, are gridded averages of *in situ* measurements at the earth's surface. Therefore, any agreement between both type of measurements would

indicate the underlying presence of an industrialization-related process that has decadal timescale effects over a vertical extent well in excess of the atmospheric boundary layer (ABL).

3. ADDITIONAL VERIFICATION – INDUSTRIALIZATION SIGNATURES IN ECMWF AND NCEP REANALYSIS DATA

In order to confirm our findings, we analyzed both the European Centre for Medium Range Weather Forecast (ECMWF) and the National Center for Environmental Prediction (NCEP) reanalysis data sets for the period 1979–2001 (Kalnay *et al*., 1996; ECMWF, 2004; NCEP, 2004).

Figure 2 shows the result of applying the thresholding method to the ECMWF and NCEP reanalysis data. We show results for both the 1000 (surface) and 500 hPa (∼5 km) altitudes. At 1000 hPa, both data sets show approximately the same behavior as the surface and satellite data, namely, an increase in temperature change corresponding to an increase in CO_2 emission threshold values. Note that the global mean trends for both reanalysis data sets (rightmost end of the blue curve) are smaller than the global mean CRU surface trend, yet larger than the global mean MSUlt trend. In passing, we note that the CRU data do not cover most of the polar regions.

The correlation between surface CO_2 emissions and temperature trends at 500 hPa is weak. Furthermore, global mean trends at 500 hPa are close to zero for both reanalysis data sets, which is consistent with the global mean trends from the MSU satellite observations. This finding – which is in line with independent radiosonde observations of free tropospheric temperatures as recently summarized by Seidel *et al*. (2004) – in combination with the clear relationship between industrialization and decadal temperature trends from the MSU satellite observations suggests that an anthropogenic non-GHG warming process directly related to industrialization has been an important forcing in the lower troposphere during the period under consideration.

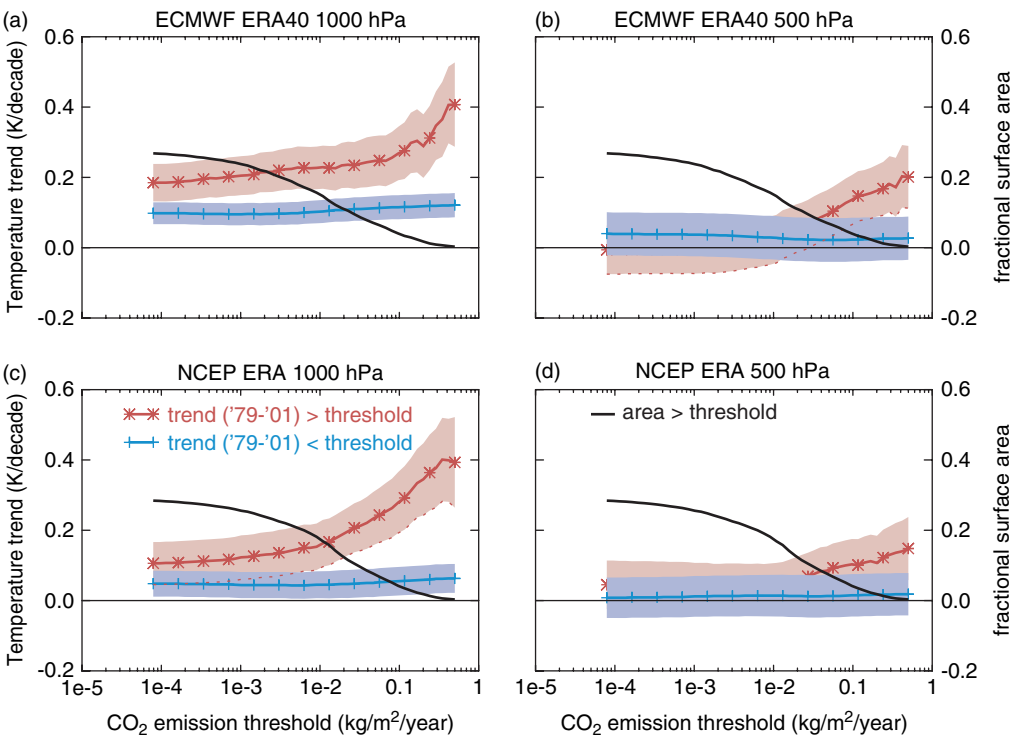

Figure 2. CO_2 emission–thresholded mean temperature trends (K/decade) as in Figure 1 but this time for reanalysis data ECMWF ERA40 1000 hPa temperature trends (a), ECMWF ERA40 500 hPa temperature trends (b), NCEP ERA 1000 hPa temperature trends (c) and NCEP ERA 500 hPa temperature trends (d). This figure is available in colour online at www.interscience.wiley.com/ijoc

4. ROBUSTNESS OF THE OBSERVED SIGNAL: STATISTICAL APPROACH AND TEMPORAL AND SPATIAL TRENDS

In this section, we consider two ways of evaluating the relationship between the real temperature trends and the way in which we have sampled the data. Our goal here is to exclude the possibility that the observed correlation is an artifact of the spatial-thresholding method. First we explore the spatial-thresholding technique and its robustness in some detail. We then attempt to isolate a more direct relationship between the thresholded CO_2 emissions and temperature in order to see if a similar correlation (temperature trend enhancements corresponding to increasing CO_2 emissions) can be observed.

4.1. Spatial sampling

We start by pointing out that the spatial-thresholding method is expected to be intrinsically robust because it involves a mixed subsampling in space. This mixed subsampling arises because different levels of CO_2 emissions correspond to discontiguous regions of the globe. Therefore, any comparison of decadal temperature trends for such spatially disconnected subsamples will largely exclude all but the most persistent spatial trends. In order to generate a confidence limit for the thresholded trend method, we use the bootstrap principle (Efron and Tibshirani, 1993). Random subsets (locations) consisting of 1/3 of the entire gridded datasets are chosen and this subset is then randomly redistributed where every individual time series is returned to the data set at a different location. This method provides confidence limits for the robustness of the spatial patterns in the dataset. This exercise was performed 1000 times for both the MSUlt and CRU data sets. The 99th percentiles of the range of thresholded trends at each CO_2 emission threshold were then taken to represent confidence limits. Figure 3(c) and (d) shows a cumulative plot for the 1000 bootstrap-sampled sets – derived from the original data sets in Figure 3(a) and (b) – along with the resulting mean and confidence limits at each CO_2 emission threshold. Clearly, the process of bootstrap sampling does not destroy the increasing slope for thresholded trend values found in the real data sets. The resulting confidence limits are smaller than the shaded regions in Figure 3(a) and (b) (the shaded regions are due to trend uncertainty) for the CO_2 emissions. Furthermore, the uncertainties in the below-threshold trends are negligible compared to the trend uncertainty. Perhaps more importantly, it is quite clear that the observed correlation between temperature trends and CO_2 emissions is not an artifact of the spatial sampling technique but reflects, instead, a persistent, underlying, spatially correlated process in the data.

4.2. Direct correlation between binned CO_2 emissions and measured temperature trends

We have so far established that a correlation exists between spatially thresholded temperature trends and the CO_2 emission threshold values themselves. Clearly, the spatial sampling of the thresholding method ensures that the mean trends appear to be quite smoothly varying functions of the threshold. In fact, the method is very similar to the concept of globally averaged mean temperature commonly found in climate studies, except that the average is taken over regions rather than over the entire globe. Perhaps the main advantage of the thresholding method is that the mean temperature trend for the above-threshold regions can be compared to the below-threshold mean temperature trends. Certainly, from the analysis presented earlier in this section it is possible to conclude that the difference in trends between these two regions is a robust indicator for a heating process, which differs between the two kinds of regions. In order to confirm robustness, we investigate the direct relationship between binned, rather than thresholded, CO_2 emissions and temperature trends.

In Figures 4 and 5, we show results of the binned trend analyses (i.e. no thresholding) for different CO_2 emission bins (chosen to be at 35 equally spaced intervals on a logarithmic scale) both for the MSUlt and CRU data as well as for the reanalysis (ECMWF and NCEP) data sets. Figure 4(b) and (d) show the number of grid points in each CO_2 emission bin used to construct Figure 4(a) and (c). There is indeed a general increase in temperature trends with increasing CO_2 emissions visible in both the MSUlt and CRU data. Furthermore, one should note that the uncertainties in the trend calculations become larger for emission bins with few grid points, especially at the lower end of the CO_2 emissions range. This is an additional indication (1) that the correlation is not caused by the thresholding method and (2) that it provides strong evidence for

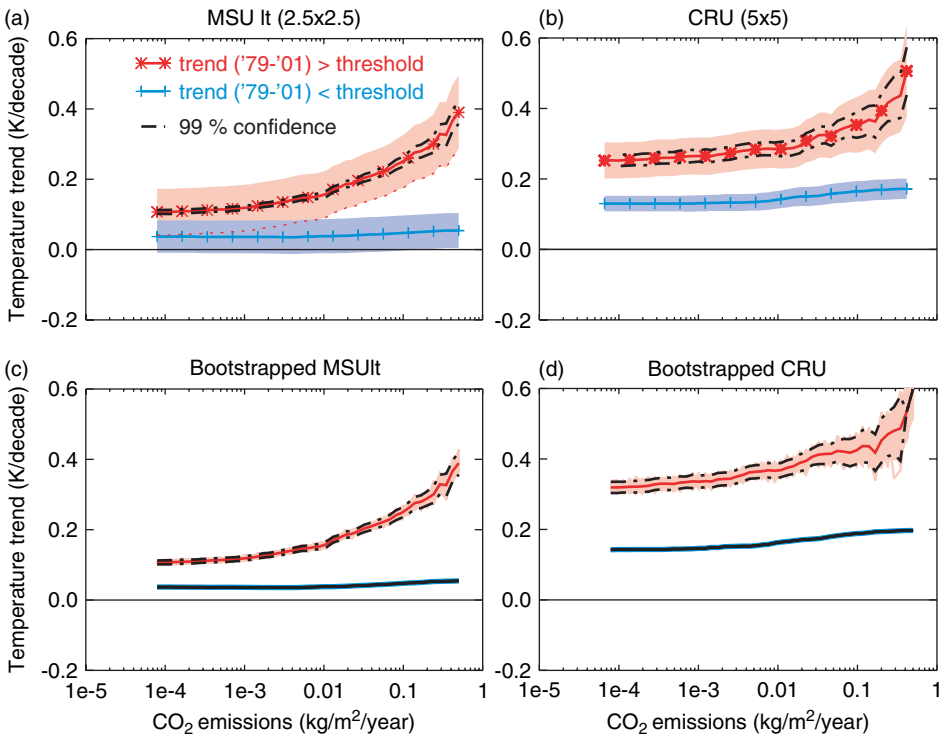

Figure 3. Robustness evaluation of the thresholding method using bootstrap sampling (see text for full explanation). The upper panels (a and b) show the results from the thresholding method for both the MSUlt and the CRU data sets (solid red line (∗): above-CO_2 emission threshold temperature trend; blue line (+): below-threshold temperature trend), including the 1-σ uncertainty from the linear regression calculation (light red and blue shaded areas) as well as 95% confidence limits (black dashed lines) taken from the bootstrapping shown in the lower panels. The lower panels show the 1000 bootstrap-resampled realizations mentioned in the text and the 95% confidence limits derived from a probability density function of the bootstrap resampling at each threshold level (dashed-dotted lines). Note that the below-threshold 95% confidence limits were too small to be distinguished from the mean trends. This figure is available in colour online at www.interscience.wiley.com/ijoc

the existence of a process linking anthropogenic CO_2 emissions directly to temperature trends. In order to test for discretization errors, we performed the same analysis with more emissions intervals (Figure 4(e) and (f)). The results are now noisier, as expected, especially for the CRU data set (Figure 4(f)), where a relationship becomes harder to discern although for the MSUlt data the relationship is still clear (Figure 4(e)).

4.3. Area dependence

In particular, Figure 4 shows that the satellite measurements appear to be more coherent that the surface measurements. This is not surprising considering that the satellite measurements are horizontal and vertical temperature averages, whereas the surface temperatures are based on point measurements that are considered to be representative for a grid cell. Individual *in situ* point measurements of surface temperature can be affected by many surface processes, complicating the interpretation of temperature variations. On the other hand, the presence of very similar industrial CO_2 emission–temperature trend correlation in different data sets indicates that these variations are robust and are important on a global scale.

A consequence of the possible influence of industrial activity on surface temperatures is that this activity probably manifests itself on regional and local scales even though it is local in origin. The presence of this correlation may therefore depend on the area that the measurement represents. To test this hypothesis, the thresholding method as well as the more direct binning method used in Section 4.2 were repeated for different grid sizes of both the satellite measurements and industrial CO_2 emissions. Figure 6 shows that the direct correlation between industrial CO_2 emissions and temperature trends is less well defined with larger

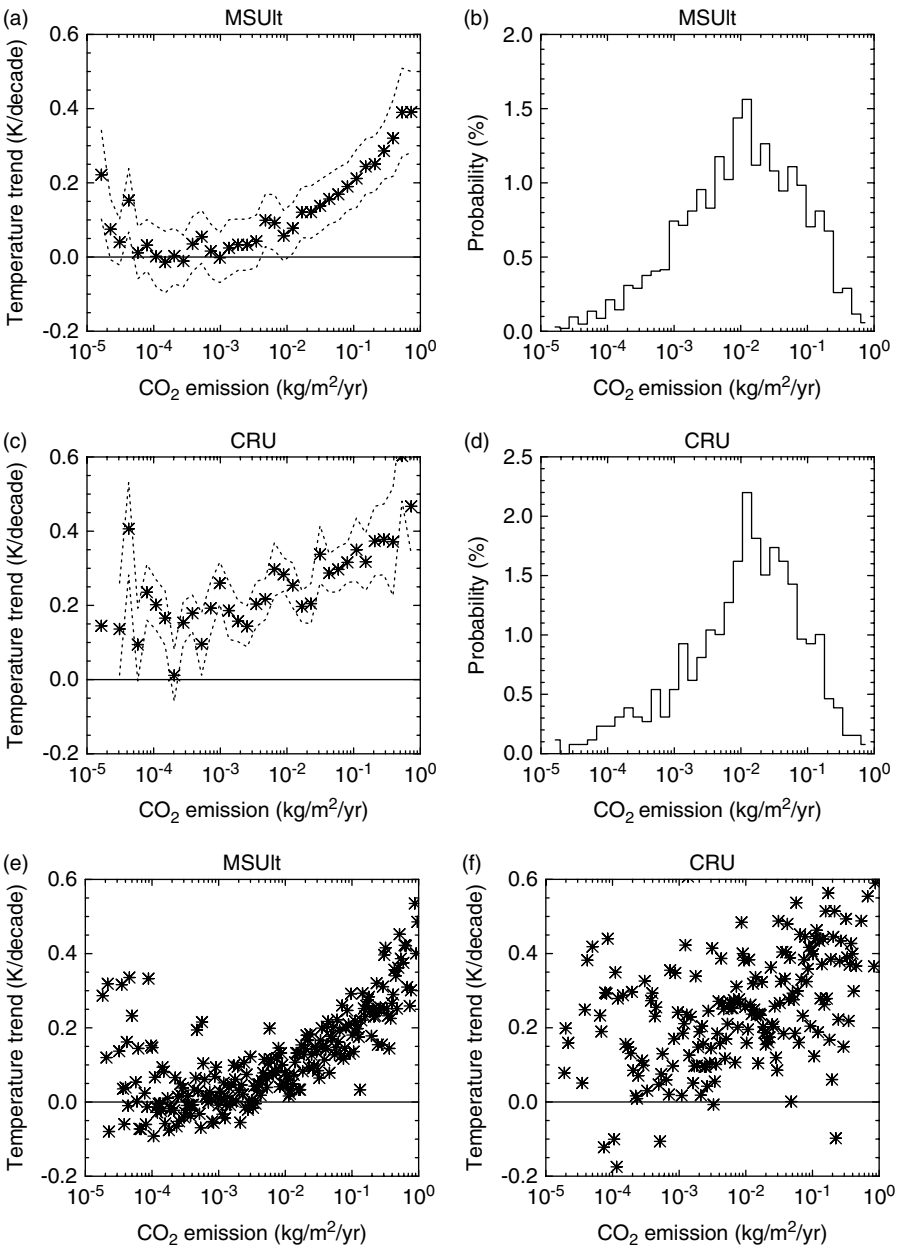

Figure 4. Mean temperature trends (1979–2001) as a function of industrial CO_2 emissions for: MSUlt (a) and CRU (c) with 35 CO_2 emission intervals and MSUlt (e) and CRU (f) with 249 CO_2 emission intervals. Note that the data has *not been thresholded* as in other figures in this work in order to confirm a direct relationship between CO_2 emissions and temperature increase. Panels (b) and (d) show the respective MSUlt and CRU grid point distributions for different CO_2 emissions. The dotted lines in panels a and c indicate the 1-σ uncertainty of the linear regression applied to the temperature observations

grid sizes. Larger grids will include more ocean areas, where temperature trends on average are lower than over land. As a result, the area coverage in Figure 6(a), (c) and (e) increases with increasing grid size and the temperature trends become noisier. For the thresholding trends (Figure 6(b), (d) and (f)), the correlation appears to be largely independent of grid size, indicating that on average this process affects a considerable part of the globe. It can therefore be concluded that this process acts on a local scale but affects temperatures on global scales.

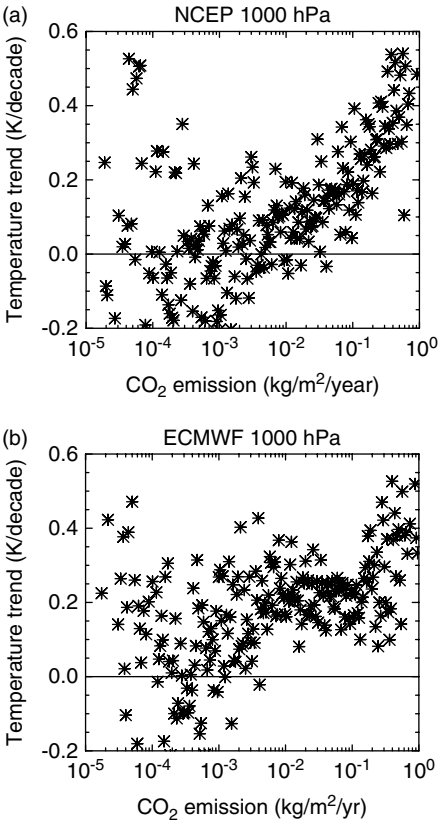

Figure 5. Similar to Figure 4, (e) and (f), but for the NCEP and ECMWF reanalyses

4.4. Latitudinal trends

It is a simple fact that most industrialized regions are found at middle and northern hemispheric latitudes. Therefore, one could expect that CO_2 emissions generally increase from south to north. Given that the Northern Hemisphere (NH) has warmed more than the Southern Hemisphere (SH) by about 0.15 K/decade over the last two decades (IPCC, 2001), it is conceivable that above-threshold temperature trend increases might be linked to the latitudinal dependence of CO_2 emissions. We find that when we apply the thresholding method to the MSUlt data for both hemispheres separately (Figure 7), the slopes of the above-threshold trends for each hemisphere in all data sets are strikingly similar for CO_2 emissions thresholds up to about 0.01 kg/m^2/year. All surface data sets (i.e. CRU, ECMWF and NCEP) show approximately the same behavior in the NH, with the warming increasing from about 0.2 to 0.4 K/decade. However, they do not show the same behavior as seen for the satellite data in the SH (note e.g. in Figure 7 the much smaller industrial CO_2 emission area coverage for the SH compared to the NH). There is also a similar slight increase in thresholded temperature trends in all data sets up to about 0.01 kg/m^2/year. Above this value, the thresholded trends either increase more rapidly (all NH data and MSUlt SH) or decrease quite rapidly (all SH data except for MSUlt). A possible explanation for these (non-MSUlt) SH trend decreases is the lack of a dense surface data network in the SH, which could lead to biases in temperature trends. In summary, the CRU data suggests that a substantial southern hemispheric warming has occurred. From the ECMWF data, it appears that only a small warming has occurred, while according to the NCEP data the SH has cooled considerably. At the moment, it is not at all clear why these differences exist. One possible explanation for the differences in our findings might, thus, be that the NCEP reanalysis does not use surface measurements while the ECMWF reanalysis does, though only in an indirect way through soil flux calculations.

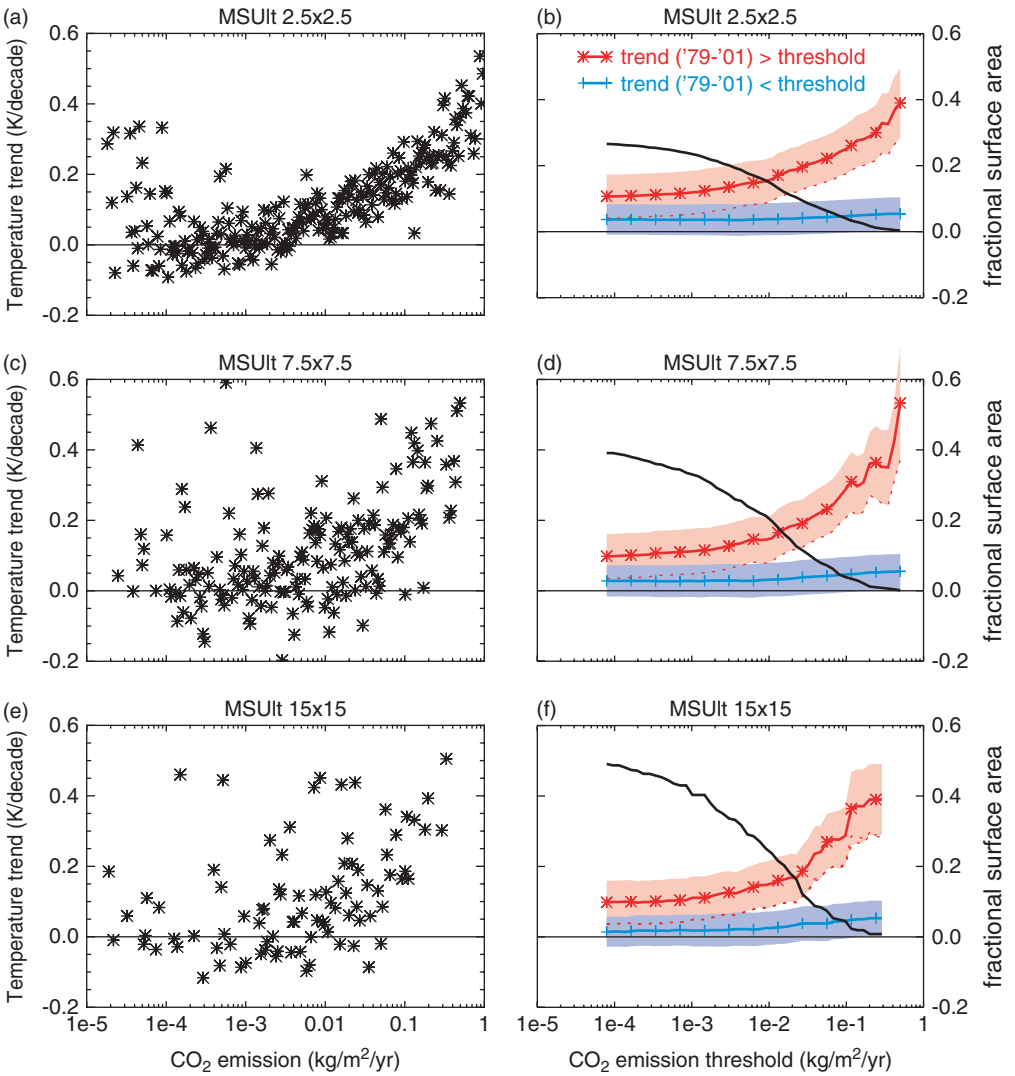

Figure 6. Panels a and b are similar to Figures 4(e) and 1(b) respectively. Panels (c) to (f) present analyses similar to those in (a) and (b), but for (c) and (d) the grid size is 7.5° × 7.5° and for (e) and (f) the grid size is 15° × 15°. This figure is available in colour online at www.interscience.wiley.com/ijoc

In addition, we mention here that there has been speculation of MSU satellite measurements having biases when measuring temperature over sea ice (Swanson, 2003). However, Christy and Norris (2004) showed by direct comparisons with radiosondes over these regions that there was no sea ice impact on correlations and trends.

4.5. Seasonality

Industrial activity takes place on the earth's surface (mostly in the NH) and, therefore, it can be expected that any physical process linked to industrialization will primarily affect temperatures in the ABL. However there are distinct differences in ABL structure between the different seasons at midlatitudes for continents (generally: a convective and deep ABL during summer, a shallow and stable ABL during winter). Therefore, we can expect that the near-surface temperature response is different when caused by processes related to industrialization. It is thus important to investigate the seasonality of temperature trends in both the CRU and MSUlt measurements

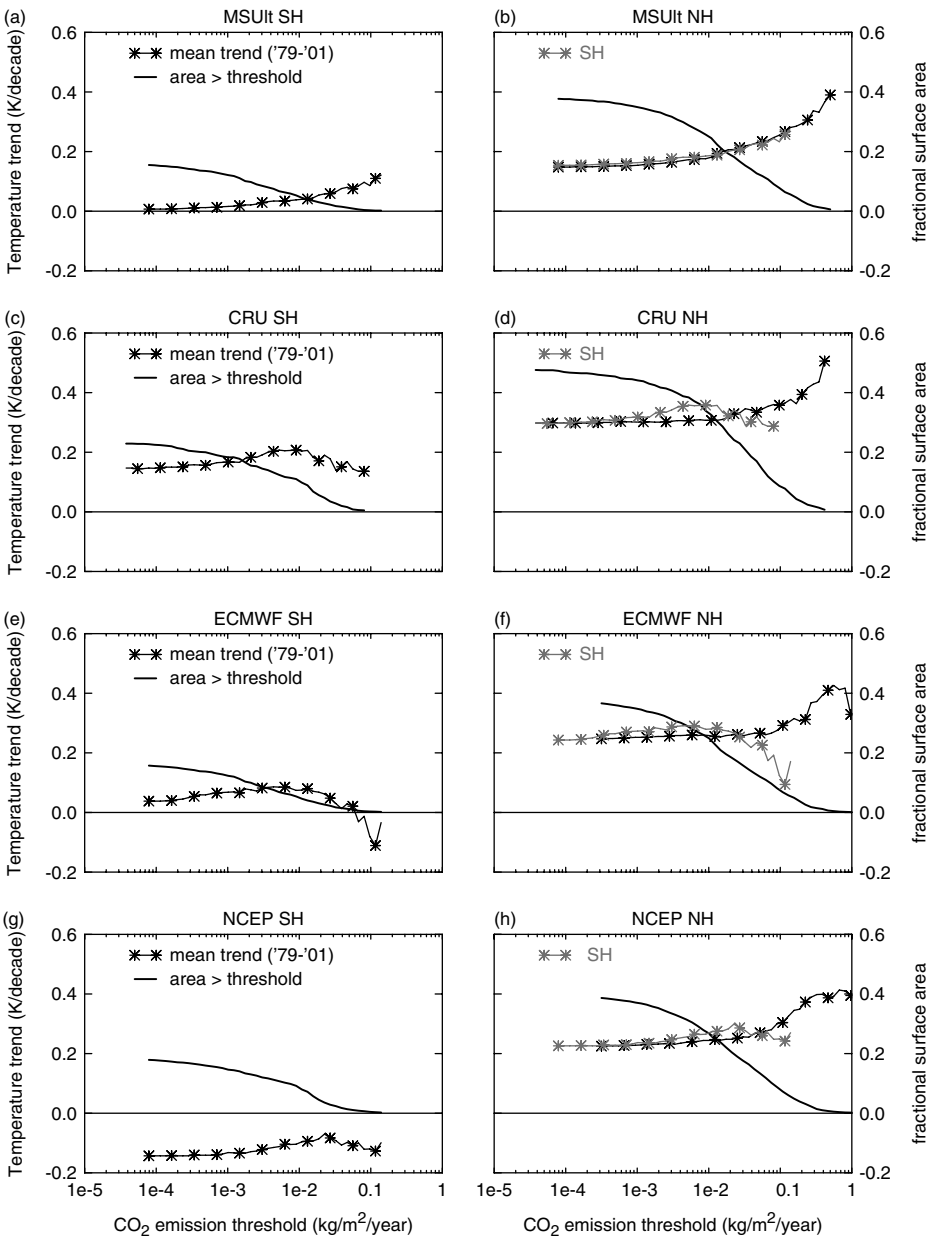

Figure 7. Mean temperature trends (K/decade) for the period 1979–2001 for different industrial CO_2 emission (kg/m^2/year) thresholds for both the Northern (b, d, f, h) and Southern (a, c, e, g) Hemispheres determined using the thresholding method for the above-threshold CO_2 emissions only. The data sets used are: MSUlt (a, b); CRU (c, d); ECMWF ERA40 1000 hPa (e, f); NCEP ERA 1000 hPa (g, h). Industrial surface CO_2 emissions are taken as usual from the EDGAR 1990 database. The gray lines in the right-hand panels indicate the southern hemispheric temperature CO_2 emission correlation from the corresponding left-hand panels, adjusted so that the mean temperature trends at the lowest CO_2 emissions values are the same. Also shown in each panel is the fractional surface area (thick solid line) for which industrial surface CO_2 emissions are larger than the threshold emissions value

for the periods December–January–February (DJF; NH winter), March–April–May (MAM; NH spring), June–July–August (JJA; NH summer) and September–October-November (SON; NH autumn).

Figure 8 shows the results of applying the thresholding method to different seasons for two different data sets. The thresholded CRU data (Figure 8(a)) shows that the strongest increase in thresholded temperature

trends occurs during NH winter and that lower increases are found during NH spring and summer. No significant increase can be identified for NH autumn. A similar pattern is found in the MSUlt data (Figure 8(b)), albeit that the magnitude of the temperature trend changes is significantly smaller. As noted before, the MSUlt measurements are sensitive to the lower troposphere and thus to both the surface and free troposphere. Therefore, the amplitude of the measured warming is expected to appear less pronounced in MSUlt data than in the CRU data because the free troposphere has warmed less than the surface. Note that both data sets show the strongest thresholded temperature trends during NH winter, in accordance with IPCC (2001). We can also see by comparing Figure 8(c) with 8(e) or Figure 8(d) with 8(f) that the global signal is dominated by the NH. For the CRU SH data, the largest temperature trends are found during NH summer (local winter) and the smallest temperature trends are found during NH winter (local summer). Our interpretation of these differences is that the ABL is more stable and shallower during local midlatitude winter compared to local summer. In other words, the heat will be trapped longer in the ABL during local midlatitude winter, and the trends will increase. During local summer, convection will be more effective in transporting the surplus heat from the ABL to the free troposphere, reducing the near-surface warming. Thus, the seasonality in temperature trends in the measurements is quite consistent with heating from surface industrialization-related processes. Note that the same kind of process could explain the difference between daytime and nighttime surface temperature changes. During the night, a stable ABL prevails, suppressing vertical exchange of heat in the ABL. During the day, the ABL is generally thicker; hence, the surface heating could be distributed over a thicker atmospheric layer. This could result in a larger temperature increase during night compared to during the day and, thus, a reduced diurnal temperature cycle. Additionally, this would be very much in agreement with the observed reduction of the amplitude of the diurnal cycle of surface temperatures (Easterling *et al*., 1997).

4.6. Correlation between CO_2 emissions and temperature trends in climate model results

In Paper I, the thresholding method was also applied to surface temperatures from two climate model simulations of GHG warming that were used in the IPCC TAR report (2003). The models used were the NCAR-DOE-PCM model and the ECHAM-OPYC. The comparison showed that measured spatial patterns were not simulated by both climate models. In this section, the same model data is analyzed in addition to what has been shown in Section 4.2. Figure 9 shows the comparison between binned industrial CO_2 emissions and modeled temperature trends similar to Figures 4 and 5. Temperature trends were calculated for both a 40-year period (2000–2039) and a 100-year period (2000–2099). Clearly, no correlation exists between industrial CO_2 emissions and temperature trends, while modeled trends are higher in both simulations when calculated for the longer period. These results are in agreement with the findings from Paper I and further emphasize the hypothesis that non-GHG anthropogenic processes (surface albedo, soil moisture, soot, clouds) may be involved in causing an increase in surface/lower tropospheric temperatures. We note in passing that our findings that middle latitudes are typically where the highest temperature trends are found (since industrial CO_2 emissions are at their largest at middle latitudes rather than at the polar regions) are quite inconsistent with the expectation of strong temperature trends at high latitudes, which is the hallmark of GHG-driven temperature trends.

5. SUMMARY AND DISCUSSION

In this work, we have established that the correlation between observed near-surface temperature trends and CO_2 emissions presented in de Laat and Maurellis (2004) occurs in a variety of data sets in a completely consistent way, indicating that the correlation is reproducible.

We have also shown that the correlation between emissions and temperature is neither an artifact of the thresholding method nor the consequence of latitudinal variations in temperature trends. The correlation may be easily recovered from a more direct comparison of emissions and temperature measurements, using binning rather than thresholding, although the binning approach is quite noisy and less well defined when using larger

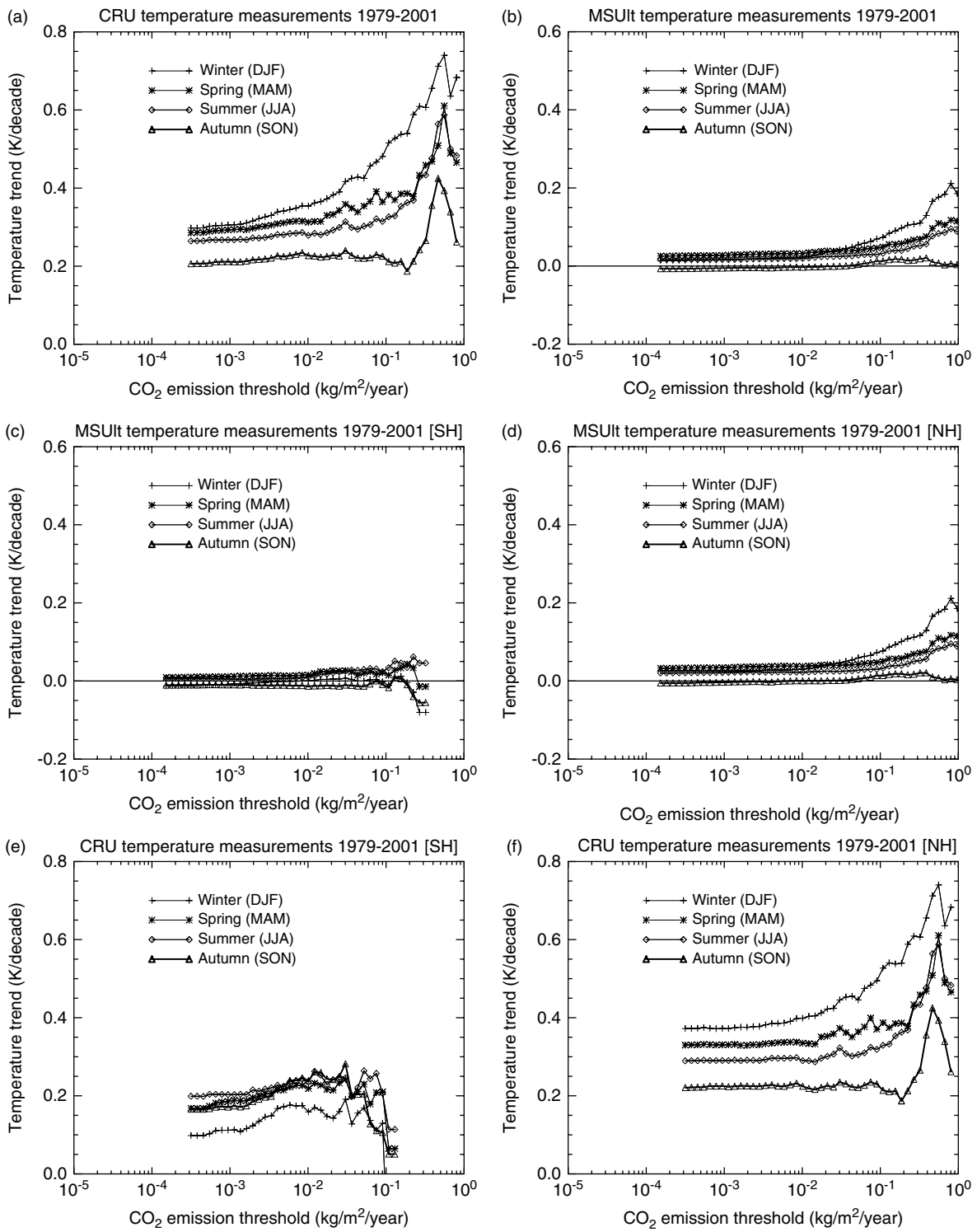

Figure 8. Seasonality of the above-threshold temperature CO_2 emission correlation using the thresholding method for the entire CRU (a) and MSUlt (b) data set, as well as for the MSUlt Southern Hemisphere (c), CRU Southern Hemisphere (d), MSUlt Northern Hemisphere (e) and CRU Northern Hemisphere (f) subsets. The seasons are defined as: DJF = December–January–February; MAM = March–April–May; JJA = June–July–August; SON = September–October–November

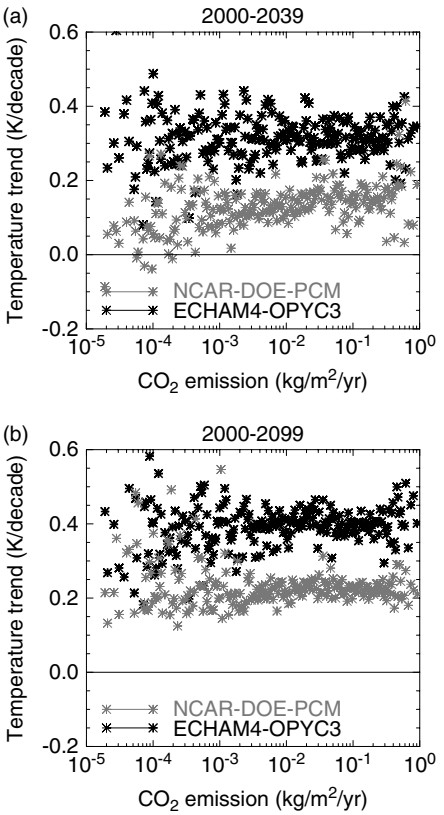

Figure 9. Climate model-simulated 2-m temperature changes using the same direct binning approach shown in Figures 4 (e and f) and 5. The temperature trends (K/decade) are calculated for the periods 2000–2039 (gray asterisks) and 2000–2099 (black asterisks) for the IPCC-IS92a emission scenario ('business as usual') using the NCAR-DOE-PCM and ECHAM4-OPYC3 climate models

grid sizes. The latter is especially true for the surface data. Perhaps more importantly, the strength of the spatial-thresholding method is that it reveals the same correlation independent of the grid spacing.

Our analysis of climate model simulations of GHG warming confirms our earlier results (Paper I), namely, that they do not show any kind of CO_2 emission–temperature trend correlation. In fact, the modeled temperature trends are quite insensitive to the magnitude of the industrial CO_2 emissions. It is possible that the response of the climate system to enhanced GHG radiative forcing is much more localized than expected in that it occurs only in specific regions and mainly in the lower troposphere, although this runs contrary to the current understanding of GHG-related processes (*cf* Hansen *et al*., 1997; IPCC, 2001; Hansen *et al*., 2005; Santer *et al*., 2005). From our findings, it is evident that the temperature trend enhancements are quite large and cover a sizable fraction of the globe (∼10%, see Figure 1). Therefore, our findings provide an additional spatial test to be satisfied by climate models in addition to the more traditional goals of reproducing historical global mean, hemispheric and free tropospheric temperature trends.

One implication is that any analysis of climate signals should consider non-GHG anthropogenic processes. In particular, our results show that both the surface and the satellite measurements (e.g. Figure 1) display the same kind of temperature trend enhancements. It is possible that the cumulative effects of small-scale human activities could contribute to lower tropospheric heating on regional or even larger scales (e.g. Hinkel *et al*. (2003)). This is not to be confused with the issue of whether the proximity of human activity may affect the local temperature measurement without changing the actual temperature over a larger surrounding (*cf* Loveland and Belward, 1997; Peterson, 2003). The act of homogenizing the data set by 'removing' urban stations from temperature data sets could in fact remove an important source of regional warming, especially in highly industrialized regions.

Recently, Block *et al*. (2004) investigated the influence of 'anthropogenic heat' on surface temperatures, which is released by densely populated industrialized areas using a (regional) climate model. The proposed physical mechanism is that energy – which is consumed in large quantities in these areas – is a conserved quantity in any physical system, and at some point this energy will be released into the atmosphere in the form of a direct near-surface temperature (energy) perturbation. By way of illustration, the average energy consumption for Germany is 1.3 Wm^{-2}, for Japan it is 2.9 Wm^{-2}, for the Netherlands it is almost 4 Wm^{-2}, while for certain industrialized regions it can easily be 20–70 Wm^{-2} (IIASA, 2003; Crutzen, 2004). Temperature perturbations of up to 0.9 K were found by Block *et al*. (2004) for a 90-day simulation of a constant surface flux of 2 Wm^{-2} over Europe's land areas, which suggest that the significant regional temperature trend enhancements discussed in this work and in Paper I could be partly explained by this process. In general, the presence of surface warming processes would require a better understanding of the structure of the ABL (both during the day and night), the effect of surface processes on it and the possibility that it affects much larger regions through advection and transport. A certain degree of seasonality exists in that surface temperature trends tend to be higher during local winter, especially for the NH, which emphasizes the importance of understanding the seasonality of the ABL. However, the physics and dynamical behavior of e.g. the stable (nighttime) ABL are currently not particularly well understood (Holtslag *et al*., 2004).

Anthropogenic heat is not the only process that can or may explain the correlation between temperature trends and industrial CO_2 emissions. There are a few other possible processes that may play a role: changes in land use that could change the surface albedo and also soil moisture and thus the surface energy balance and also groundwater levels; absorbing aerosols like soot, cloud cover or cloud optical properties all are potentially plausible explanations. Natural causes can also not be excluded at the moment, although at first instance they are less probable because of the large spatial variations in industrial CO_2 emissions.

Finally, we point out that it seems unreasonable to assume that the 'classical' urban heat island (different heating due to different land cover) is the cause of the enhanced surface warming over industrialized regions since the area coverage of urbanized regions is far too small to explain the spatial extent of the regional temperature trend enhancements discussed in this paper.

ACKNOWLEDGEMENTS

We would particularly like to thank all institutions and organizations cited in this work for making their data publicly available (IPCC, ECMWF, NCAR, RIVM, RSS, UK Meteorological Office/Hadley Centre and University of Alabama, Huntington).

APPENDIX

1. A NOTE ON SPATIAL THRESHOLDING ANALYSIS UNITS

In Paper I, the increase in temperature trend with increasing thresholded CO_2 emissions was smaller in the CRU surface observations than in the MSUuah data. However, the units used in Paper I were absolute CO_2 emissions (kg/year), which do not take into account the area size of the grids. It is thus somewhat unfair to compare one data set at $2.5^\circ \times 2.5^\circ$ resolution (MSU) with a data set at $5^\circ \times 5^\circ$ resolution (CRU) using total CO_2 emissions as the highest total CO_2 emissions will be larger for a CRU grid point compared to a MSU grid point. Figure A1 in the appendix compares the temperature trends using the thresholding method applied to CO_2 measured in Paper I units (Tg) and total CO_2 emissions per grid (kg/year). For the MSUlt data, the maximum CO_2 emission limit goes up to 30 Tg/grid point, whereas for the CRU data the CO_2 emissions are as high as 120 Tg/grid point (Figure A1a). Figure A1b shows the results of the thresholding method when scaling the CO_2 emissions with the surface area of the grid (kg/m^2/year). Now, both trend analyses are directly comparable and are much more similar. The most significant remaining difference is the smaller mean trend in the MSUlt data, which, as explained above, could be related to the lower weighting of lower tropospheric temperatures in the MSUlt data. However, the pattern of stronger warming over more

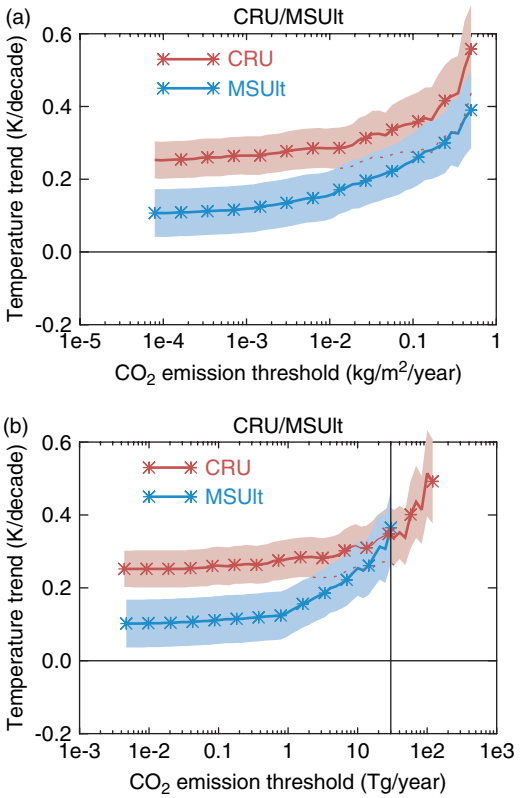

Figure A1. Mean above CO_2 emission–thresholded temperature trends (K/decade) covering the period 1979–2001 for different industrial CO_2 emission thresholds using the total amount per grid (kg/year; (b), as used in Paper I) and the grid-area weighted amount (kg/m^2/year; (b), as used in this work) for lower tropospheric MSU satellite temperature trends (MSUlt, blue line) and surface temperature trends from the Hadley Center/Climate Research Unit data set (CRU, red line). Industrial surface CO_2 emissions are taken from the EDGAR 1990 database. The shaded areas denote the mean 1-σ uncertainties of the linear regressions, which do not include measurement errors for the MSUlt data. The vertical black line indicates the highest CO_2 emission value used in that figure. The left panel may be compared with Figure 1(a) and (b). This figure is available in colour online at www.interscience.wiley.com/ijoc

industrialized regions is obvious in both data sets and thus appears to be a robust signature of temperature variations. In the remainder of this paper, we will use only the area-weighted CO_2 emissions (in units of kg/m^2/year).

2. SENSITIVITY OF SATELLITE MEASUREMENTS TO SURFACE TEMPERATURES

In Paper I, we showed that there exists a positive correlation between spatially thresholded industrial CO_2 emissions (EDGAR database; van Aardenne *et al*., 2001) and observed temperature trends. For that analysis, we used both satellite data (MSU middle and lower troposphere temperature measurements (Christy *et al*. 2003) referred to as the MSUuah and MSUlt data sets; MSU middle troposphere (Mears *et al*. 2003) referred to hereafter as the MSUrss data set) and gridded surface measurements (Hadley Centre/CRU historical gridded surface temperature data set (Jones and Moberg 2003) hereafter the CRU data set, which is based on *in situ* surface measurements). Middle tropospheric temperatures are measured by MSU channel 2. Although all data sets showed evidence for a general increase in temperature trend when spatially thresholded against increasing CO_2 emissions, the surface trends were higher than the satellite-measured lower tropospheric temperature trends. This discrepancy need not be a cause for concern since, as will be shown here, the MSU instruments are less sensitive to positive near-surface temperature trends

In order to illustrate this, we only have to consider the weighting functions of the satellite measurements (Christy *et al*., 2003). Assuming that the ABL (with a thickness of 1 km) shows a warming of 0.2 K (close to the actually observed surface warming trend) with no other atmospheric temperature trends, the satellite measurements would show a warming trend of about 0.035 and 0.01 K/decade for the MSU lower and middle tropospheric measurements respectively. Furthermore, for a warming trend of 0.2 K throughout the troposphere (height = 15 km), those numbers would be about 0.2 and 0.18 K respectively. Our simple calculation yields values for the middle and lower tropospheric temperature trends, which are comparable to what has been reported in Christy *et al*. (2003). But more importantly, this calculation clearly shows that *measured* tropospheric trends that are small can only result from free tropospheric temperature trends that are small.

REFERENCES

Bengtsson L, Roeckner E, Stendel M. 1999. Why is the global warming proceeding much slower than expected. *Journal of Geophysical Research* **104**: 3865–3876.

Block A, Keuler K, Schaller E. 2004. Impacts of anthropogenic heat on regional climate patterns. *Geophysical Research Letters* **31**: L12211 DOI:10.1029/2004GL019852.

Chase TN, Pielke RA Sr, Herman B, Zeng X. 2004. Likelihood of rapidly increasing surface temperatures unaccompanied by strong warming in the free troposphere. *Climate Research* **25**: 185–190.

Christy JR, Norris WB. 2004. What may we conclude about global tropospheric temperature trends? *Geophysical Research Letters* **31**: L06211, DOI:10.1029/2003GL019361.

Christy JR, Spencer RW, Norris WB, Braswel W. 2003. Error estimates of version 5.0 of MSU-AMSU Bulk Atmospheric temperatures. *Journal of Atmospheric and Oceanic Technology* **20**: 613–629.

Covey C, AchutaRao KM, Cubasch U, Jones P, Lambert SJ, Mann ME, Phillips TJ, Taylor KE. 2003. An overview of results from the Coupled Model intercomparison project. *Global and Planetary Change* **37**: 103–133.

Crutzen PJ. 2004. New directions: The growing urban heat and pollution "island" effect – impact on chemistry and climate. *Atmospheric Environment* **38**: 3539–3540.

de Laat ATJ, Maurellis AN. 2004. Industrial CO_2 emissions as a proxy for anthropogenic influence on lower tropospheric temperature trends. *Geophysical Research Letters* **31**: L05204 DOI:10.1029/2003GL019024.

Easterling RE, Horton B, Jones PD, Peterson TC, Karl TR, Parker DE, Salinger MJ, Razuvayev V, Plummer N, Jamason P, Folland CK. 1997. Maximum and minimum temperature trends for the globe. *Science* **277**: 364–367.

ECMWF. www.ecmwf.int, ECMWF ReAnalysis 1957–2002 (ERA40), 2004.

Efron B, Tibshirani RJ. 1993. *An Introduction to the Bootstrap*. Chapman and Hall: New York.

Gaffen DJ, Santer BD, Boyle JS, Christy JR, Graham NE, Ross RJ. 2000. Mutidecadal changes in the vertical temperature structure of the tropical troposphere. *Science* **287**: 1242–1245.

Hansen J, Ruedy R, Lacis A, Russell G, Sato Mki, Lerner J, Rind D, Stone P. 1997. Wonderland climate model. *Journal of Geophysical Research* **102**: 6823–6830.

Hansen J, Sato M, Ruedy R, Nazarenko L, Lacis A, Schmidt GA, Russell G, Aleinov I, Bauer M, Bauer S, Bell N, Cairns B, Canuto V, Chandler M, Cheng Y, Del Genio A, Faluvegi G, Fleming E, Friend A, Hall T, Jackmann C, Kelley M, Kiang N, Koch D, Lean J, Lerner J, Lo K, Menon S, Miller R, Minnis P, Novakov T, Oinas V, Perlwitz Ja, Perlwitz Ju, Rind D, Romanou A, Shindell D, Stone P, Sun S, Tausnev N, Tresher D, Wielicki B, Wong T, Yao M, Zhang S, Efficacy of climate forcings, *Journal of Geophysical Research* **110**: DOI:10.1029/2005JD005776, D18104, 2005.

Hinkel KM, Nelson FE, Kleine AE, Bell JH. 2003. The urban heat island in winter at Barrow, Alaska. *International Journal of Climatology* **23**: 1889–1905.

Holtslag AAH GEWEX Atmospheric Boundary Layer Study (GABLS), www.gewex.org/gabls.htm, 2004.

IIASA, International Institute for Applied Systems Analysis, http://www.iiasa.ac.at/Research/TNT/WEB/heat/, 2003.

IPCC (Intergovernmental Panel for Climate Change). Houghton JT (ed). *Climate Change 2001: The Scientific Basis*, Cambridge University Press: New York, 2001.

Jones PD, Moberg A. 2003. Hemispheric and large-scale surface air temperature variations: An extensive revision and an update to 2001. *Journal of Climate* **16**: 206–223.

Kalnay E, Kanamitsu M, Kistler R, Collins W, Deavan D, Iredell M, Saha S, White G, Woolen J, Zhu Y, Leetmaa A, Reynolds R, Chelliah M, Ebisuzaki W, Higgins W, Janowiak J, Mo KC, Ropelewski C, Wang J, Jenne R, Joseph D. 1996. The NCEP/NCAR 40-year reanalysis project. *Bulletin of the American Meteorological Society* **82**: 247–267.

Lanzante JR, Klein SA, Seidel DJ. 2003. Temporal homogenization of monthly radiosonde temperature data. Part II: trends, sensitivities and MSU comparison. *Journal of Climate* **16**: 241–262.

Loveland TR, Belward AS. 1997. The IGBP-DIS global 1 km land cover data set, DISCover: first results. *International Journal of Remote Sensing* **18**: 3289–3295.

Mears C, Schabel M, Wentz FJ. 2003. A reanalysis of the MSU channel 2 tropospheric temperature record. *Journal of Climate* **16**: 3650–3664.

NCEP. NCEP/NCAR reanalysis project, www.cdc.noaa.gov/ncep_reanalysis/, 2004.

Pepin NC, Seidel DJ. 2005. A global comparison of surface and free-air temperatures at high elevations. *Journal of Geophysical Research* **110**: DOI:10.1029/2004JD005047.

Peterson TC. 2003. Assessment of Urban versus Rural in Situ surface temperatures in the contiguous United States: No difference found. *Journal of Climate* **16**: 2941–3071.

Santer BD, Wigley TML, Boyle JS, Gaffen DJ, Hnilo JJ, Nychka D, Parker DE, Taylor KE. 2000. Statistical significance of trends and trend differences in layer-average atmospheric temperature time series. *Journal of Geophysical Research* **105**: 7337–7356.

Santer BD, Wigley TML, Mears C, Wentz FJ, Klein SA, Seidel DJ, Taylor KE, Thorne PW, Wehner MF, Gleckler PJ, Boyle JS, Collins WD, Dixon KW, Doutriaux C, Free M, Fu Q, Hansen JE, Jones GS, Ruedy R, Karl TR, Lanzante JR, Mehl GA, Ramaswamy V, Russell G, Schmidt GA. Amplication of surface temperature trends and variability in the tropical atmosphere, *ScienceExpress*, DOI:10.1126/science.1114867, 2005.

Seidel DJ, Lanzante JR. 2004. An assessment of three alternatives to linear trends for characterizing global atmospheric temperature changes. *Journal of Geophysical Research* **109**: D14108 DOI:10.1029/2003JD004414.

Seidel DJ, Angell JK, Christy J, Free M, Klein SA, Lanzante JR, Mears C, parker D, Schabel M, Spencer R, Sterin A, Thorne P, Wentz F. 2004. Uncertainty in signals of large-scale climate variations in radiosonde and satellite upper-air temperature datasets. *Journal of Climate* **17**: 2225–2240.

Swanson RE. 2003. Evidence of possible sea-ice influence on Microwave Sounding Unit tropospheric temperature trends in polar regions. *Geophysical Research Letters* **30**: 2040 DOI:10.1029/2003GL017938.

van Aardenne JA, Dentener FJ, Olivier JGJ, Klein Goldewijk CGM, Lelieveld J. 2001. A $1^\circ \times 1^\circ$ resolution data set of historical anthropogenic trace gas emissions for the period 1890–1990. *Global Biogeochemical Cycles* **15**(4): 909–928.

